



University of Groningen

Zinc(II) tetraphenylporphyrin on Au(111) investigated by scanning tunnelling microscopy and photoemission spectroscopy measurements

De Luca, Oreste; Caruso, Tommaso; Grimaldi, Ilenia; Policicchio, Alfonso; Formoso, Vincenzo; Fujii, Jun; Vobornik, Ivana; Pacile, Daniela; Papagno, Marco; Agostino, Raffaele Giuseppe

Published in:
Nanotechnology

DOI:
[10.1088/1361-6528/ab95ba](https://doi.org/10.1088/1361-6528/ab95ba)

IMPORTANT NOTE: You are advised to consult the publisher's version (publisher's PDF) if you wish to cite from it. Please check the document version below.

Document Version
Publisher's PDF, also known as Version of record

Publication date:
2020

[Link to publication in University of Groningen/UMCG research database](#)

Citation for published version (APA):

De Luca, O., Caruso, T., Grimaldi, I., Policicchio, A., Formoso, V., Fujii, J., Vobornik, I., Pacile, D., Papagno, M., & Agostino, R. G. (2020). Zinc(II) tetraphenylporphyrin on Au(111) investigated by scanning tunnelling microscopy and photoemission spectroscopy measurements. *Nanotechnology*, 31(36), [365603]. <https://doi.org/10.1088/1361-6528/ab95ba>

Copyright

Other than for strictly personal use, it is not permitted to download or to forward/distribute the text or part of it without the consent of the author(s) and/or copyright holder(s), unless the work is under an open content license (like Creative Commons).

Take-down policy

If you believe that this document breaches copyright please contact us providing details, and we will remove access to the work immediately and investigate your claim.

Downloaded from the University of Groningen/UMCG research database (Pure): <http://www.rug.nl/research/portal>. For technical reasons the number of authors shown on this cover page is limited to 10 maximum.

PAPER • OPEN ACCESS

Zinc(II) tetraphenylporphyrin on Au(111) investigated by scanning tunnelling microscopy and photoemission spectroscopy measurements

To cite this article: Oreste De Luca *et al* 2020 *Nanotechnology* **31** 365603

View the [article online](#) for updates and enhancements.




IOP | ebooks™

Bringing together innovative digital publishing with leading authors from the global scientific community.

Start exploring the collection—download the first chapter of every title for free.

Zinc(II) tetraphenylporphyrin on Au(111) investigated by scanning tunnelling microscopy and photoemission spectroscopy measurements

Oreste De Luca^{1,2,5} , Tommaso Caruso^{1,2,3}, Ilenia Grimaldi¹, Alfonso Policicchio^{1,2,3}, Vincenzo Formoso^{1,2,3}, Jun Fujii⁴, Ivana Vobornik⁴, Daniela Pacilé¹, Marco Papagno¹ and Raffaele Giuseppe Agostino^{1,2,3}

¹ Dipartimento di Fisica, Università della Calabria, 87036, Arcavacata di Rende(CS), Italy

¹ CNR-Nanotec, UoS di Cosenza, Dipartimento di Fisica, Università della Calabria, 87036, Arcavacata di Rende (CS), Italy

³ Consiglio Nazionale Interuniversitario Scienze Fisiche della Materia (C.N.I.S.M), Via della Vasca Navale, 84, 00146, Roma, Italy

⁴ INFN, CNR, TASC Lab, I-34012, Trieste, Italy

E-mail: o.de.luca@rug.nl

Received 6 March 2020, revised 14 May 2020

Accepted for publication 22 May 2020

Published 22 June 2020



CrossMark

Abstract

Porphyrins are a versatile class of molecules, which have attracted attention over the years due to their electronic, optical and biological properties. Self-assembled monolayers of porphyrins were widely studied on metal surfaces in order to understand the supramolecular organization of these molecules, which is a crucial step towards the development of devices starting from the *bottom-up* approach. This perspective could lead to tailor the interfacial properties of the surface, depending on the specific interaction between the molecular assembly and the metal surface. In this study, we revisit the investigation of the assembly of zinc-tetraphenylporphyrins on Au(111) in order to explore the adsorption of the molecular network on the noble metal substrate. The combined analysis of scanning tunneling microscopy (STM) imaging and core levels photoemission spectroscopy measurements support a peculiar arrangement of the ZnTPP molecular network, with Zn atoms occupying the bridge sites of the Au surface atoms. Furthermore, we prove that, at few-layers coverage, the interaction between the deposited layers allows a relevant molecular mobility of the adlayer, as observed by STM and supported by core levels photoemission analysis.

Supplementary material for this article is available [online](#)

Keywords: self-assembled monolayer, porphyrin, STM, photoemission spectroscopy, gold surface

(Some figures may appear in colour only in the online journal)

⁵ Present address: Zernike Institute for Advanced Materials, University of Groningen, 9747, AG, Groningen, The Netherlands



Original content from this work may be used under the terms of the [Creative Commons Attribution 4.0 licence](#). Any further distribution of this work must maintain attribution to the author(s) and the title of the work, journal citation and DOI.

1. Introduction

Assemblies of molecular architectures on metal surfaces are intriguing systems due to the possibility of synthesizing advanced functional nanostructured materials and devices through molecular manipulation. The structure and stability of a well-ordered two-dimensional adlayer are essentially determined by the compromise between the molecule-molecule and molecule-surface interactions, though other effects, such as the surface reconstruction, can play an important, and often underestimated, role. The interaction between the molecules and the surface can affect the shape of the adsorbed molecules [1] and their electronic structure [2–4], as well as their magnetic properties [5, 6]. In particular, the deposition of electron donor or acceptor molecules allows to create interfaces with well-defined electronic properties. Among organic molecules used in surface self-assembly studies, porphyrins are a well-known and versatile class of molecules, which have attracted the attention over the last years for their significant electronic, optical and biological properties exploitable in a wide range of emerging technologies including field-effect transistors [7, 8], dye-sensitized solar cells [9, 10], sensors [11, 12], organic light emitting diode [13, 14] and synthetic bio-mimetic devices [15, 16]. A noteworthy porphyrin derivative is tetraphenylporphyrin (TPP), consisting of a porphyrin macrocycle with four phenyl groups bound to the pyrrole subunits by a carbon bridge. TPP molecules, with or without the metal transition atom (Fe, Co, Ni, Cu, Zn) in the center, exhibit a pronounced self-assembling behavior on noble metal surfaces such as Au(111) [17–22], Ag(111) [23, 24] and Cu(111) [25–27], as well as on TiO₂ [28] even at room temperature. As a result of the adsorption, these molecules typically form a stable molecular packing driven by the in-plane interaction between the phenyl groups, resulting typically in a nearly square unit cell, where the porphyrin macrocycle stays either flat and parallel on the metal surface or distorted, showing the typical saddle-shape geometry, as reported by several Scanning Tunneling Microscopy (STM) and Near Edge x-Ray Absorption Fine Structure (NEXAFS) studies [25, 29–33].

In the present work, we revisit the deposition of the Zinc(II) tetraphenylporphyrin (ZnTPP) (see molecular structure in figure 1) on the Au(111) surface by means of STM and photoemission from core levels. Although this system was already studied by STM [17, 18, 20], the adsorption of the molecular assembly on the noble metal surface needs further attention. Our STM measurements on single layer ZnTPP evidence a highly ordered molecular network allowing to identify the unit cell vectors of the system, as well as strong dis-homogeneity in the local charge distribution. These results, supported by photoemission experiments are in contrast with previous results [18], and may be explained in term of a peculiar adsorption geometry of the ZnTPP on the Au(111) surface. Furthermore, for higher molecular coverages, STM analysis shows that the second layer of the ZnTPP molecules is epitaxially formed on the first one. A weak interaction between the first layers is proved by diffusion effects first observed on this system, as

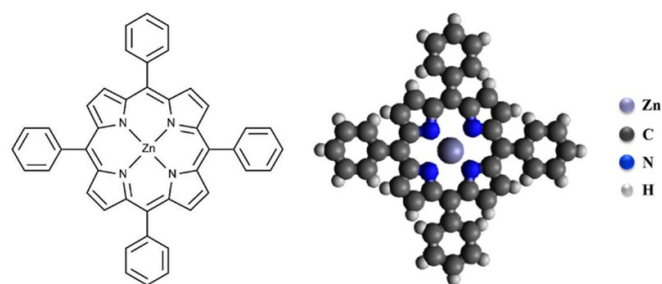


Figure 1. Molecular structure of the ZnTPP molecule, which exhibits the zinc at the center of the macrocycle, and four phenyl groups.

well as by the evolution of photoemission spectra in the few-layer regime.

2. Experimental section

STM measurements were performed at ‘Laboratorio Idruri Metallici’ (SPES Group, Department of Physics, Università della Calabria, Italy) at room temperature (RT) and in UHV conditions (base pressure of 5×10^{-10} mbar) with an Aarhus SPM 150 equipped with KolibriSensor™ from SPECS [34] and with a Nanonis Control system. The sharp STM W-tip was cleaned *in situ* via Ar⁺ sputtering. STM images were also acquired at the APE beamline (Elettra Synchrotron Light Source, Italy), at room temperature and in UHV condition (base pressure of 1×10^{-10} mbar), with a home-built STM, priorly to photoemission measurements. In the STM images shown, the tunneling bias voltage (U_t) is referred to the sample, whereas the tunneling current (I_t) is that collected at the tip. All STM images were processed using the WSxM software (8.3 version) [35] and by a home-made routine for the determination of mesh averaged images. We note that all the presented STM results were reproduced in two different experimental setups.

All core levels and valence band spectra were recorded at room temperature and in normal emission geometry. Photoemission data have been normalized to the background after the subtraction of a Shirley function. The Au(111) surface (Phasis, Au(111) on mica with 200 nm of thick gold layer, 99.99% purity), was cleaned by several cycles of Ar⁺ sputtering ($I_{\text{sample}} = 6 \mu\text{A}$ for 20 min) followed by annealing ($T = 723 \text{ K}$ for 20 min). The cleanliness quality of the pristine gold surface was verified with both STM and photoemission measurements. ZnTPP molecules (Porphyrin Systems, Zn(II) meso-tetraphenylporphine >98% purity) were deposited at room temperature on Au(111) by organic molecular beam deposition at a pressure of 3×10^{-8} mbar using a home-built evaporator. The evaporation temperature range was 553 K–573 K, while the deposition rate was set to 1 monolayer/10 min (here 1 monolayer (ML) is the molecular coverage necessary to fully cover the substrate). The monolayer coverage was obtained by a single dose deposition of ZnTPP molecules on Au(111), while few-layers coverage samples

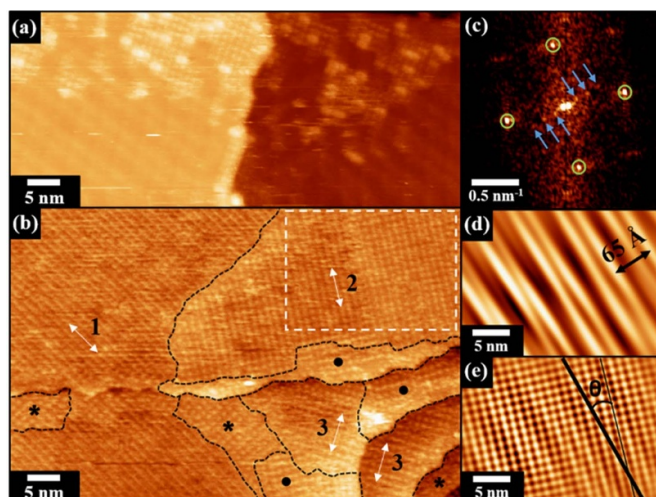


Figure 2. (a) $85 \times 36 \text{ nm}^2$ RT-STM image of ZnTPP/Au(111) at submonolayer coverage ($\sim 0.4 \text{ ML}$). Tunneling parameters: $U_t = 0.95 \text{ V}$, $I_t = 0.1 \text{ nA}$. (b) $85 \times 56 \text{ nm}^2$ RT-STM image depicting three main rotated domains (labelled 1, 2 and 3) of ZnTPP on Au(111). The white two-headed arrows mark the direction of one molecular axis unit cell. Additional domains (labelled * and •) are also observed. The molecular coverage is $(1.1 \pm 0.1) \text{ ML}$. Tunneling parameters: $U_t = 1.2 \text{ V}$, $I_t = 0.1 \text{ nA}$. (c) Fourier analysis of the region enclosed by the white rectangular box in panel (b). Blue arrows and green circles highlight the diffraction spots relative to the herringbone (panel (d)) and of the molecular assembly (panel (e)).

were the results of distinct depositions of different molecular doses, starting from the monolayer deposition. The samples at sub-monolayer coverage consisted of a single molecular dose deposition of ZnTPP at surface. All molecular coverages were estimated by measuring the intensity ratio between the N 1s and Au 4f photoemission peaks, through comparison with the corresponding STM images at the monolayer regime.

3. Results and discussion

The Au(111) surface was carefully characterized by STM, priorly to ZnTPP deposition. The pristine sample surface presents flat and large terraces, up to 200 nm, separated by steps of about 2.3 \AA in height (see figure S1(a) in the supplementary material (available at stacks.iop.org/Nano/31/365603/mmedia)). High-resolution STM images reveal the typical long-range herringbone reconstruction of the Au(111) surface (see figure S1(b) in the supplementary material). It is known that the energy of the surface layer is reduced by formation of periodic regions in which Au atoms occupy alternatively face-centered-cubic (fcc) and hexagonal closed-packed (hcp) sites, with the former being energetically more favorable [36]. In the interface between these regions, Au atoms occupy bridge-sites which appear as bright stripes (called soliton walls or discommensuration lines) in the STM image (see inset of figure S1(b) in the supplementary material).

Figure 2(a) presents an STM image collected by depositing a submonolayer of ZnTPP on Au(111) surface. The molecules form mainly single-layer islands characterized by a

highly ordered and well-defined assembly. Interestingly, relatively small brighter regions of second layer ZnTPP are also observed. At submonolayer coverages ($0.3\text{--}0.4 \text{ ML}$), the number of molecules of the second layer islands is about 10% of the first layer molecules. By increasing the amount of deposited ZnTPP, the molecular islands grow their lateral size and start to coalesce until the whole metallic surface is covered by about one monolayer, as shown in figure 2(b). Three distinct main domains are observed (labelled 1, 2 and 3) rotated one with respect to the other by $30^\circ \pm 2^\circ$ (see figure S2 in the supplementary material). Additional ZnTPP domains (marked with * and • in figure 2(b)) rotated by about 90° with respect to the main ones are also observed. The underlying herringbone structure cannot be resolved due to the positive bias voltage between the STM tip and the sample. However, through Fourier analysis (see figure 2(c)), it is possible to visualize the herringbone reconstruction beneath the molecular network, as displayed in figure 2(d). The spacing between two equivalent soliton walls is $(65 \pm 3) \text{ \AA}$, in agreement with previous works [37–39]. In addition, we can estimate the angle $\theta = 19^\circ \pm 2^\circ$ between the soliton walls and the major axis of the molecular lattice (see figure 2(e)).

Figure 3(a) shows a high-resolution STM image for $(1.1 \pm 0.1) \text{ ML}$ of a single-domain ZnTPP on Au(111). This measurement proves that the molecules self-assemble in a molecular pattern with a nearly square unit cell. The lattice parameters of the molecular network, estimated by means of a statistical analysis on the self-correlated pictures (see figure S3 in the supplementary material), are $a = (14.0 \pm 0.2) \text{ \AA}$, $b = (13.6 \pm 0.2) \text{ \AA}$ and $\theta = 89.0^\circ \pm 0.8^\circ$ (density: $0.53 \text{ molecules nm}^{-2}$), in good agreement with previous works [17, 18, 20]. Figure 3(b) presents a mesh averaged image from the STM data shown in figure 3(a), *i.e.* obtained by summing over several unit cells of the overlayer ZnTPP molecules lattice (more than 70 single unit cell in the present case) by taking into account its periodicity. This procedure increases the signal to noise ratio of the STM measurement allowing a detailed identification of the molecule's contour. In particular, the pyrrole subunits of each molecule can be easily identified, along with the T-shape (perpendicular) bonding between adjacent molecules [17–19]. For the tunneling parameters here used (positive bias voltages), the STM probes the empty electronic states. Since each Zn ion has filled d states ($3d^{10}$) centred at about 10 eV binding energy (see discussion below), the contribution of the metal ions to the tunneling current is expected to be irrelevant at $\sim 1 \text{ eV}$ below the Fermi level, causing the Zn ions to appear as a dark spots at the centre of the ZnTPP molecule [18, 20]. Though, for a proper understanding of the metallic ion contrast as a function of the bias voltage, the interaction between the Zn ion and the macrocycle, the substrate, and the STM tip must be considered [40, 41]. On the other hand, we are able to prove that the pyrrole subunits of the molecules macrocycle exhibit different contrast, with the four subunits displaying distinct intensity. This result implies a loss of the molecular D_{4h} symmetry when adsorbed on the Au(111) surface. This non-homogeneity of the local charge distribution may result by a peculiar interaction between the metallic substrate and the organic molecules,

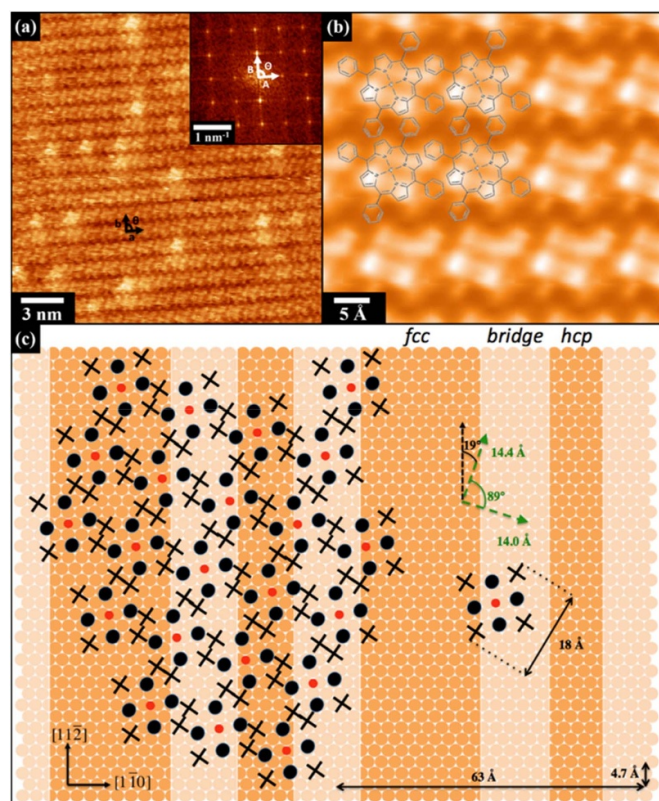


Figure 3. (a) $25 \times 25 \text{ nm}^2$ RT-STM image of (1.1 ± 0.1) ML of ZnTPP on Au(111). a , b and θ are the unit cell parameters. Tunneling parameters: $U_t = 0.9 \text{ V}$, $I_t = 0.1 \text{ nA}$. Inset: FFT analysis of the STM acquisition; A , B and Θ are the lattice parameters in the reciprocal space. (b) Mesh averaged molecular layer image gained by STM acquisitions; the ZnTPP molecular model is superimposed on it. (c) Model of the Au(111) reconstructed surface along with the ZnTPP molecular assembly. In the schematic representation of the ZnTPP molecules, red dots represent Zn atoms, full circles the pyrrole groups, and crosses the phenyl units.

but may also stems from a specific molecular adsorption geometry. Though previous study [18] suggests that the centre of ZnTPP molecules occupy the top site of Au surface atoms with the pyrrole and phenyl groups located in hollow sites, we propose here a different adsorption configuration supported by our results.

In figure 3(c) we present a sketch of the Au(111) surface with ZnTPP molecules adsorbed. To simulate the surface reconstruction, the next-nearest neighbour (NNN) distance of the Au atoms has been compressed by 4.4% along the $[1\bar{1}0]$ direction with respect to the NNN distance in bulk atoms [37–39]. The herringbone unit cell has thus vectors of 63 \AA and 4.7 \AA in the $[1\bar{1}0]$ and $[11\bar{2}]$ direction, respectively. The soliton walls are represented by white stripes running parallel to the $[11\bar{2}]$ direction. Assuming the dimension of the adsorbed molecules as the one of the free molecule, 18 \AA , by taking into account the experimental misorientation angle (19°) between the major axis of the molecules and the soliton walls, and the size of the unit cell vectors, we have tested several possible adsorption geometries. From this analysis we infer that the only configuration which is consistent with the STM findings, is to position the Zn atoms on the bridge-sites of

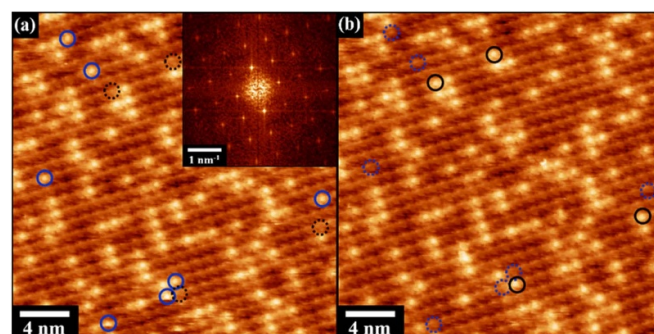


Figure 4. (a)–(b) Consecutive RT-STM images of the same $30 \times 30 \text{ nm}^2$ area of ZnTPP on Au(111); the molecular coverage was (1.3 ± 0.1) ML and the tunneling parameters $U_t = 1.1 \text{ V}$, $I_t = 0.1 \text{ nA}$. The inset in (a) is the Fourier analysis of the corresponding image.

the Au surface atoms (see figure 3(c)). The proposed molecular network has a unit cell vectors that differ by less than 3% from the experimental ones. In this configuration, the four pyrrole groups occupy non-equivalent sites. This finding, may well explain the non-homogeneity of the local charge distribution of pyrrole subunits observed in figure 3(b). On the other hand, the phenyl units are found close to the hollow sites.

Both figure 2(b) for the submonolayer case and figure 3(a) for a 1.1 monolayer case, evidence second layer molecules imaged as bright spots on top of the first layer lattice, which increase in number with the amount of the deposited molecules. Figure 4(a) presents an STM image for (1.3 ± 0.1) ML of ZnTPP showing that second layer molecules grow epitaxially over the first layer. Each second layer molecule is in fact found on top of a molecular site of the first layer. A cross-sectional profile along the molecules of the first and second layers is shown in figure S4 (see the supplementary material). The well-defined spots of Fourier analysis (see inset in figure 4(a)) confirms that the first and second molecular layer share the same lattice parameters. For what concerns the interaction between the first and the second layer of ZnTPP, the STM images collected one after the other on the same sample area and shown in figures 4(a) and (b) demonstrate that 2nd layer molecules moved to a different position after the first image was collected, as indicated by the black/blue circles in figure 4, pointing to van der Waals interaction.

Although the diffusion phenomenon is well-known and widely studied for organic molecules at metal surfaces [42, 43], to the best of our knowledge, this is the first time that this effect is observed for this particular system. We further note that the tip-surface interaction can favour the molecular diffusion [44–48]; however, in this work, the tunneling parameters used during the STM acquisitions are not expected to destabilize the molecular overlayer.

To investigate more in detail the molecule-substrate system, we have carried out photoemission experiments as a function of molecular coverage (from the sub-monolayer regime up to about 3 ML of thickness). In this context, the N 1s core level peak can provide useful information concerning the ZnTPP adsorption configuration and possible distortions, as four N atoms are bound to the central metal ion as well as

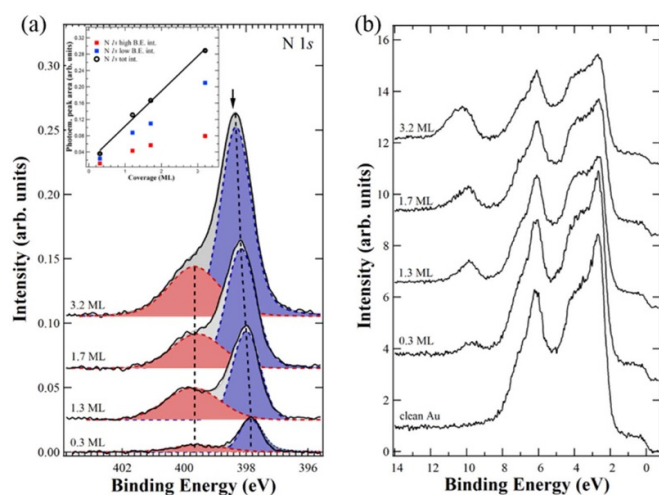


Figure 5. (a) N 1 s photoemission peaks as a function of the ZnTTP coverage on Au(111). In the inset, quantitative analysis of N 1 s components as a function of molecular coverage. All photoemission spectra were fitted by using Voigt profile shapes, after Shirley background subtraction; (b) valence band spectra of clean and ZnTTP-covered Au(111). N 1 s and valence band spectra were taken at 510 eV and 450 eV, respectively, of photon energy.

to the carbon ring skeleton (see figure 1). Figure 5(a) shows the evolution of the N 1 s state as a function of ZnTTP coverage. Already in the sub-monolayer regime (~ 0.3 ML), the N 1 s peak is split into two main broad components separated by about 1.8 eV, as opposed to weakly-interacting ‘thick’ molecular films of ZnTTP where a single component centered at 398.5 eV of binding energy (BE) is found [31]. The feature at lower binding energy (blue in figure 5(a)) exhibits a shift from 397.8 eV at ~ 0.3 ML to about 398.3 eV at (3.2 ± 0.1) ML. We ascribe this shift to an improved polarization screening of the core hole in thinner films [31].

A similar shift was also observed in our systems for C 1 s spectra (see figure S5 in the supplementary material). At the highest coverage, by comparing the N 1 s BE value of the prominent component with that recorded for a thick ZnTTP film [31], we estimate a few-layer regime rather than a multilayer one. On the other hand, the higher binding energy component (red in figure 5(a)) is centered at (399.7 ± 0.2) eV regardless of the coverage, but the peak area tends towards saturation just above 1 ML coverage (red squares in the inset of figure 5(a)). In the inset of figure 5(a), we also report the N 1 s total area, displaying the expected linear trend with increasing ZnTTP coverage.

These results are similar to the adsorption of 1 ML ZnTTP molecules on Ag(110) where the two components are separated by 0.37 eV [31]. The two N 1 s components have been attributed either to a saddle-distortion of the macrocycle or to a breaking of the D_{4h} symmetry of the ZnTTP molecule, yielding different adsorption sites of N atoms on the rectangular substrate [31]. In metal free porphyrins, two well-resolved components of equal intensity separated by about 2 eV appearing the N 1 s photoemission line, attributed to aminic ($-\text{NH}-$) and iminic ($=\text{N}-$) nitrogen [49]. In analogy with these systems, we tentatively assign the two N 1 s

components in the Au(111) surface observed in the sub- and mono-layer regime to the coexistence of different chemical environments of the four nitrogen atoms within the macrocycle [25, 31], consistently with the inhomogeneous local charge distribution observed by STM. For increasing coverages, the adsorbed molecules partly recover the D_{4h} symmetry and the N 1 s line shape approaches that of a free molecule.

Figure 5(b) displays the valence band spectra of ZnTTP on Au(111) for increasing coverages. The clean Au(111) spectrum is shown for comparison as bottom curve of figure 5(b). The Zn 3d peak exhibits a relatively broad feature at all coverage similarly to ZnTPP on nanostructured TiO_2 [50]. The binding energy of the 3d states is centered at about 9.8 eV for (1.3 ± 0.1) ML ZnTPP and shifts toward higher BE for increasing coverage due to final state effects. Except for the Zn 3d photoemission states, other ZnTTP related features cannot be singularly resolved as they overlap with gold states. However, clear modifications of the substrate valence band for increasing molecular coverage are observed. In particular, the ZnTTP highest occupied molecular orbitals at ~ 2.0 eV and the mesophenyl-related structures at ~ 3.0 eV [51] affect the energy and line-shapes of the Au structures in the energy range between 2.0 and 6.0 eV (see figure S6 in the supplementary material).

4. Conclusion

In this work, the deposition of ZnTTP molecules on the Au(111) substrate was revisited by using a combination of STM imaging and core levels photoemission measurements. We have shown that ZnTTP forms highly ordered and well defined assembly on the Au(111) surface. Through a detailed investigation we were able to determine the lattice parameters of the molecular network and estimate the misorientation angle between the major axis of the molecules and the soliton walls. These results allowed us to determine the ZnTTP adsorption geometry showing a peculiar arrangement of the ZnTTP molecular network, with Zn atoms occupying the bridge sites of the Au surface atoms. Photoemission from core levels performed as a function of the molecular coverage support the STM findings. In particular, the strong inhomogeneity of local charge distribution of the pyrrole moieties observed by STM is reflected on the line-shape and binding energy of the N 1 s structure. For higher molecular coverage, STM measurements proves that the second layer grows epitaxially with the ZnTTP monolayer. The observed molecular mobility, never reported for this specific system, suggests that the first molecular layer may act as an interface layer allowing the growth of weakly interacting additional organic layers.

Acknowledgments

This work was supported by the European Community’s Seventh Framework Program (FP7 2007-2013) through the MaTeRiA Project (PONA3 00370). The authors thank Professor P Rudolf for critical reading of the manuscript.

Conflict of interest

The authors declare no competing financial interests.

ORCID iD

Oreste De Luca  <https://orcid.org/0000-0002-4428-0863>

References

- [1] Jung T A, Schlittler R R and Gimzewski J K 1997 *Nature* **386** 696
- [2] Ruocco A, Evangelista F, Gotter R, Attili A and Stefani G 2008 *J. Phys. Chem. C* **112** 2016
- [3] Hauschild A, Karki K, Cowie B C C, Rohlfing M, Tautz F S and Sokolowski M 2005 *Phys. Rev. Lett.* **94** 036106
- [4] Romaner L, Heimel G, Brédas J L, Gerlach A, Schreiber F, Johnson R L, Zegenhagen J, Duhm S, Koch N and Zojer E 2007 *Phys. Rev. Lett.* **99** 256801
- [5] Wende H et al 2007 *Nat. Mater.* **6** 516
- [6] Gambardella P et al 2009 *Nat. Mater.* **8** 189
- [7] Seol M L, Choi S J, Kim C H, Moon D I and Choi Y K 2011 *ACS Nano* **6** 183
- [8] Noh Y Y, Kim J J, Yoshida Y and Yase K 2003 *Adv. Mater.* **15** 699
- [9] Mathew S, Yella A, Gao P, Humphry-Baker R, Curchod B F, Ashari-Astani N, Tavernelli I, Rothlisberger U, Nazeeruddin M K and Grätzel M 2014 *Nat. Chem.* **6** 242
- [10] Urbani M, Grätzel M, Nazeeruddin M K and Torres T 2014 *Chem. Rev.* **114** 12330
- [11] Ishihara S, Labuta J, Van Rossom W, Ishikawa D, Minami K, Hill J P and Ariga K 2014 *Phys. Chem. Chem. Phys.* **16** 9713
- [12] Lvova L, Di Natale C and Paolesse R 2013 *Sensors Actuators B* **179** 21
- [13] Friend R H et al 1999 *Nature* **397** 121
- [14] Fenwick O, Sprafke J K, Binas J, Kondratuk D V, Di Stasio F, Anderson H L and Cacialli F 2011 *Nano Lett.* **11** 2451
- [15] Balaban T S 2005 *Acc. Chem. Res.* **38** 612
- [16] Cosnier S, Gondran C, Wessel R, Montforts F P and Wedel M 2000 *J. Electroanal. Chem.* **488**
- [17] Zhang X L, Jiang J W, Liu Y T, Lou S T, Gao C L and Jin Q Y 2016 *Sci. Rep.* **6** 22756
- [18] Ruggieri C, Rangan S, Bartynski R A and Galoppini E 2015 *J. Phys. Chem. C* **119** 6101
- [19] Teugels L G, Avila-Bront L G and Sibener S J 2011 *J. Phys. Chem. C* **115** 2826
- [20] Yoshimoto S, Tsutsumi E, Suto K, Honda Y and Itaya K 2005 *Chem. Phys.* **319** 147
- [21] Barlow D E, Scudiero L and Hipps K W 2004 *Langmuir* **20** 4413
- [22] Deng W and Hipps K W 2003 *J. Phys. Chem. B* **107** 10736
- [23] Di Santo G et al 2011 *Chem. Eur. J.* **17** 14354
- [24] Weber-Bargioni A, Reichert J, Seitsonen A P, Auwärter W, Schiffrin A and Barth J V 2008 *J. Phys. Chem. C* **112** 3453
- [25] Brede J et al 2009 *Nanotechnology* **20** 275602
- [26] Rojas G et al 2010 *J. Phys. Chem. C* **114** 9408
- [27] Stark M, Ditze S, Drost M, Buchner F, Steinrück H P and Marbach H 2013 *Langmuir* **29** 4104
- [28] Rangan S, Ruggieri C, Bartynski R, Martínez J I, Flores F and Ortega J 2016 *J. Phys. Chem. C* **120** 4430
- [29] Mielke J, Hanke F, Peters M V, Hecht S, Persson M and Grill L 2015 *J. Am. Chem. Soc.* **137** 1844
- [30] Müllegger S, Rashidi M, Lengauer T, Rauls E, Schmidt W G, Knör G, Schöfberger W and Koch R 2011 *Phys. Rev. B* **83** 165416
- [31] Castellarin-Cudia C et al 2010 *Chem. Phys. Chem.* **11** 2248
- [32] Brede J, Linares M, Lensen R, Rowan A E, Funk M, Bröring M, Hoffmann G and Wiesendanger R 2009 *J. Vac. Sci. Technol. B* **27** 799
- [33] Yokoyama T, Yokoyama S, Kamikado T and Mashiko S 2001 *J. Chem. Phys.* **115** 3814
- [34] Torbrügge S, Schaff O and Rychen J 2010 *J. Vac. Sci. Technol. B* **28** C4E12–C4E20
- [35] Horcas I, Fernández R, Gomez-Rodriguez J M, Colchero J W S X, Gómez-Herrero J W S X M and Baro A M 2007 *Rev. Sci. Instrum.* **78** 013705
- [36] Bürgi L, Brune H and Kern K 2002 *Phys. Rev. Lett.* **89** 176801
- [37] Barth J V, Brune H, Ertl G and Behm R J 1990 *Phys. Rev. B* **42** 9307
- [38] Nie S, Bartelt N C, Wofford J M, Dubon O D, McCarty K F and Thürmer K 2012 *Phys. Rev. B* **85** 205406
- [39] Corso M, Fernández L, Schiller F and Ortega J E 2010 *ACS Nano* **4** 1603
- [40] Auwärter W et al 2010 *Phys. Rev. B* **81** 245403
- [41] Buchner F, Warnick K G, Wölffe T, Göring A, Steinrück H P, Hieringer W and Marbach H 2009 *J. Phys. Chem. C* **113** 16450
- [42] Antczak G, Kamiński W, Sabik A, Zaum C and Morgenstern K 2015 *J. Am. Chem. Soc.* **137** 14920
- [43] Weckesser J, Barth J V and Kern K 1999 *J. Chem. Phys.* **110** 5351
- [44] Li J, Berndt R and Schneider W D 1996 *Phys. Rev. Lett.* **76** 1888
- [45] Sørensen M R, Jacobsen K W and Jónsson H 1996 *Phys. Rev. Lett.* **77** 5067
- [46] Bott M, Hohage M, Morgenstern M, Michely T and Comsa G 1996 *Phys. Rev. Lett.* **76** 1304
- [47] Ebert P, Lagally M G and Urban K 1993 *Phys. Rev. Lett.* **70** 1437
- [48] Bürker C, Franco-Cañellas A, Broch K, Lee T L, Gerlach A and Schreiber F 2014 *J. Phys. Chem. C* **118** 13659
- [49] Chen M, Feng X, Zhang L, Ju H, Xu Q, Zhu J, Gottfried J M, Ibrahim K, Qian H and Wang J 2010 *J. Phys. Chem. C* **114** 9908
- [50] Castellarin-Cudia C et al 2015 *J. Phys. Chem. C* **119** 8671
- [51] Mo Y W 1993 *Phys. Rev. Lett.* **71** 2923